

# Cooling and Trapping of Fröhlich Polaron and Observation of Plasma Formation in Magnetic Field

Njutapmvoui Adamou<sup>1</sup>, Mwebi Ekengoue Clautaire<sup>2,3,\*</sup>, Kenfack Jitsa Aurelien<sup>4</sup>,  
Kenfack Sadem Christian<sup>1,2,\*</sup>, Fotue Alain Jervé<sup>1,2</sup>, Lukong Cornelius Fai<sup>1,2</sup>

<sup>1</sup>Faculty of Sciences, University of Dschang (UDs), Dschang, Cameroon

<sup>2</sup>Division of Scientific Research and Innovations, African Scientific Association for Innovative and Entrepreneurship (ASAIE), Dschang, Cameroon

<sup>3</sup>Faculty of Engineering and Technology (FET), University of Buea (UB), Buea, Cameroon

<sup>4</sup>Faculty of Sciences, University of Yaounde I (UYI), Yaounde, Cameroon

## Email address:

clautaire.mwebiekengoue@yahoo.fr (Mwebi Ekengoue Clautaire), kevinsadem@yahoo.fr (Kenfack Sadem Christian)

\*Corresponding author

## To cite this article:

Njutapmvoui Adamou, Mwebi Ekengoue Clautaire, Kenfack Jitsa Aurelien, Kenfack Sadem Christian, Fotue Alain Jervé, Lukong Cornelius Fai. Cooling and Trapping of Fröhlich Polaron and Observation of Plasma Formation in Magnetic Field. *American Journal of Optics and Photonics*. Vol. 11, No. 1, 2023, pp. 10-19. doi: 10.11648/j.ajop.20231101.12

**Received:** July 22, 2023; **Accepted:** August 14, 2023; **Published:** November 11, 2023

---

**Abstract:** Due to their physical properties and potential importance to the understanding of the electron mobility in a wide variety of materials, polarons are currently the subject of intensive research. Using one of the world most powerful trapping entity, we investigated the influence of surrounding environment on the dynamic of Fröhlich polaron with the help of semiclassical approach under rotating wave approximation (RWA), in the consideration that we deal with a two-level-system (TLS). Both the frequency of the trap and the bandgap value between energy levels of the system particles dictate the resulting phenomenon. Trapping of Fröhlich polarons with magnetic field conducts to complete population transfer from excited state to ground state with the possibility of the formation of Bose-Einstein Condensates (BEC) at low bandgap energy values and important value magnetic field frequency. Fundamentally different to polaritons, nomatter the breaking down of Pauli Exclusion Principle (BDPEP), the magnetic trapping of quasiparticles Fröhlich polarons conducts to plasma formation when both the bandgap value of energy levels and the magnetic field frequency are very important. Detailed analysis of the resulted phenomenon will open a new perspectives toward understanding the dynamic of cooled and trapped Fröhlich polarons.

**Keywords:** Polarons, Magnetic Field, Trapping, Semiclassical Approach, Bose-Einstein Condensates, Plasma Formation

---

## 1. Introduction

Quantum physics [1] is based on a set of mathematical concepts and equations. It requires an adequate physical interpretation [1]. Both theoretical and practical exploitation of quantum physics have open door to other subdomains including quantum communication and computation [2-4] which depend on quantum bits (Qbit) [4]. The Qbit can be placed in a continuous set of superposition of its two states [5] and therefore considered as a quantum TLS. In quantum communication and computation, Qbits are used for the encoding of information [6]. Far from being a recent area of science and technology [7], quantum information is a rapidly

growing domain of research that involves several scientific fields. The research field aims to proceed quantum information using quantum computers [8]. These are devices which provide physical implementation of quantum mechanical unitary transformations acting on an array of Qbits containing computational inputs in the form of binary labeled quantum states [9-12]. The devices transform the initial quantum superposed states into final ones [13]. The strength of quantum computer results from its properties [14].

The development of quantum computers is preceded by that of transistors which are used to construct logic gates known as the fundamental building blocks for computations and algorithms. Likewise, trapped ions are used to implement quantum logic gates. Good logic gates make use of the least

energy and operate fast. They are sensitive to small energy changes and fast fluctuations in their environment. Qbits-environment interaction stands as the origin of quantum decoherence. Thus, successful implementation of quantum computers requires the consideration of the interactions between the system and its environment. Several techniques are proposed to mitigate the issue known as decoherence problem. Some of them include the use of cryogenic cooling and error correction code [15], quantum decoherence itself [16], QLifeReducer implementation and photon-echo technique [17] to cite a few. Other different methods have been proposed by authors of Refs.[18-23]. In the Computational Condensed Matter Physics and Nanomaterials Laboratory at the University of Dchang (West-Cameroon), several research works have been carried in the same direction [24-27].

Among these research works, we find that of Refs. [26, 27] more promising in addressing decoherence problem in quantum computation. This because, the particles of consideration, trapped with magnetic field considered as a trap, have been cooled down with laser radiation at very low temperature conducting to Bose-Einstein condensates (BEC). This state of particles has been termed coherent population state by authors of Ref. [26, 27]. Motivated by this observation, we follow their theoretical approach to cold and trap Fröhlich polaron with a magnetic field which we consider as a trap, given that such a research work has not been carried before. Doing it, this paper aims to point out the advantages of using magnetic field as a trap to investigate the influence of surrounding environment on the dynamic of Fröhlich polaron.

This paper is divided into four main parts. The second part deals with the theory used to approach our problem. In this section, we use semiclassical approach under RWA to investigate the influence of the trap on the dynamic of Fröhlich polaron thereby calculating transition probability and energy. The third part presents the numerical results obtained and their discussion. Finally, the paper ends up in the fourth section with a conclusion and gives certain orientation to further research works.

## 2. Theoretical Analysis

There exist several possible Qbit implementation systems [28]. In the present study we focus our attention to the trapped-ion Qbit device which provided the first experimental demonstration of a fundamental quantum logic gate [29]. For assumption, important key points are considered. First, instead of electromagnetic trap, we consider

a magnetic trap. Second, in the trap, the ion is replaced with an electron which is looked as a TLS with ground and excited states  $|0\rangle$  and  $|1\rangle$  respectively and with corresponding energies  $E_i$  ( $i = 0, 1$ ). Next, we consider that both electron and phonon are confined in the trap, results a quasiparticle called cooled and trapped polaron. Finally, we consider the one dimensional modes. The system wavefunction  $\Psi$  is a linear superposition of electron wavefunction  $\varphi_n(r, x_n)$ , localized on the  $n^{\text{th}}$  lattice site and dependent on internuclear displacement  $\{\Psi = \sum_n a_n(x_1; x_2; x_3; \dots; x_n)\varphi_n(r, x_n)\}$ . The system's Hamiltonian is given in Eq.1.

$$H = \frac{P^2}{2m} + \sum_m \left( \frac{P_m^2}{2\mu} + \frac{1}{2} \mu \omega^2 x_m^2 \right) + \sum_m [U(r - ma, x_m)] \quad (1)$$

In Eq.1, the first and second terms to the right hand side correspond respectively to the electron kinetic energy and the n-molecule chain total energy in which the parameters  $\mu$  and  $\frac{P_m^2}{2\mu}$  indicate the reduced mass and their kinetic energy. We consider relative ion displacement to be small in such away that reciprocal interaction is taking harmonic. The last term to the right hand side of Eq.1 is known as the electron-chain ions interaction when the electron is in the  $m^{\text{th}}$  molecules. In order to determine  $a_n$  coefficients, let consider Schrödinger Eq. 2.

$$H\Psi = E\Psi \quad (2)$$

The substitution of Eq.1 into Eq.2 conducts to the eigenvalues Eq. 3 where  $\varepsilon(x_n)$  is the eigenenergies. Eq.3 represents the energy associated to an electron when there is only one molecule.

$$\left[ -\frac{\hbar^2}{2m} \nabla^2 + U(r - na, x_n) \right] \varphi_n(r, x_n) = \varepsilon(x_n) \varphi_n(r, x_n) \quad (3)$$

Following the assumptions made on  $U(r - ma, x_m)$  and  $\varphi_n(r, x_n)$ , we then obtain Eq.4 where the parameter  $J(x_n, x_m)$  expressed in Eq.5 is a superposition integral and the parameter  $W_n(x_1, x_2, x_3, \dots, x_n)$  (Eq.6) describes the perturbation on  $\varepsilon(x_n)$  due to other atomic entities in the trap.

$$\left[ \varepsilon(x_n) + \sum_m \left( \frac{P_m^2}{2\mu} + \frac{1}{2} \mu \omega^2 x_m^2 \right) + W_n(x_1, x_2, x_3, \dots, x_n) \right] a_n(x_1, x_2, x_3, \dots, x_n) + J(x_n, x_{n+1}) a_{n+1}(x_1, x_2, x_3, \dots, x_n) + J(x_n, x_{n-1}) a_{n-1}(x_1, x_2, x_3, \dots, x_n) = E a_n(x_1, x_2, x_3, \dots, x_n) \quad (4)$$

$$J(x_n, x_m) = \int dr \varphi_n^*(r, x_n) U(r - na, x_n) \varphi_m(r, x_m) \quad (5)$$

$$W_n(x_1, x_2, x_3, \dots, x_n) = \int dr \left| \varphi_n(r, x_n) \right|^2 \sum_{p \neq n} U(r - pa, x_p) \quad (6)$$

If internuclear coordinates were all blocked in the same equilibrium position  $x$ , eigen coefficients then take the standard value indicated in Eq.7 and eigenvalues of the proceeding Eq.4 are given in Eq.8, where we have choosen  $J(x_n, x_{n+1}) = -J$ , negative constant in agree with negative potential  $U$ .

$$a_n^k = e^{ikna} \quad (7)$$

$$E_k = E(x) + W_n(x_1, x_2, x_3, \dots, x_n) + \frac{N}{2} \mu \omega^2 x^2 - 2J \cos(ka) \quad (8)$$

In order to make deeper our treatment, we consider the following assumption. First, we consider that the eigenvalues  $E(x_n)$  depends linearly by  $x_n$  on  $E(x_n) = -\gamma x_n$ . Second, the parameter  $W_n(x_1, x_2, x_3, \dots, x_n)$  is negligable, since other atomic entities such as electrons and phonons lightly influence particle of consideration. Third, superposition integral is independent from internuclear coordinates  $J(x_n, x_{n+1}) = -J$ . From the above considerations, the Hamiltonian Eq.1 takes the reduced form of Eq.9 in which the parameters  $c_{i,\sigma}^*(c_{j,\sigma})$  denote electron creation (destruction) operators on site  $i(j)$  with spin  $\sigma$ .

$$H = -J \sum_{\langle i,j \rangle, \sigma} (c_{i,\sigma}^* c_{j,\sigma} + h.c) + H_P - \sum_j \gamma x_j c_j^* c_j \quad (9)$$

In Eq.9, we eliminate spin index as we are treating a single particle problem. With  $\langle i, j \rangle$  we indicate first neighbours, while with  $H_P$  we means Eq.10. Here and from Eq.9, we introduce the bosonic creation (destruction) operators who accounts for phonons Eq.11 and Eq.12 where  $N$  indicates lattice sites number.

$$H_P = \sum_m \left( \frac{P_m^2}{2\mu} + \frac{1}{2} \mu \omega^2 x_m^2 \right) \quad (10)$$

$$x_j = -\frac{1}{\sqrt{N}} \sum_q \sqrt{\frac{\hbar}{2\mu\omega}} (a_q + h.c) e^{iqR_j} \quad (11)$$

$$P_j = \frac{i}{\sqrt{N}} \sum_q \sqrt{\frac{\hbar\mu\omega}{2}} (a_q - h.c) e^{iqR_j} \quad (12)$$

From the above, Hamiltonian Eq.9 becomes as given in Eq.13 where we introduce the coupling constant

$$g = \frac{\gamma}{\hbar\omega} \sqrt{\frac{\hbar}{2\mu\omega}}.$$

$$H = - \left( J \sum_{\langle i,j \rangle, \sigma} c_j^* c_j + h.c \right) + \hbar\omega \sum_q a_q^+ a_q + \sum_{j,q} \hbar\omega g \frac{e^{iqR_j}}{\sqrt{N}} c_j^* c_j (a_q + a_{-q}^+) \quad (13)$$

If we consider Eq.14 and Eq.15 and following theoretical formalism of [30], we can obtain the final Hamiltonian form Eq.16 which corresponds to Holstein Hamiltonian.

$$c_k^+ = \frac{1}{\sqrt{N}} \sum_i c_i^+ e^{-ikR_i} \quad (14)$$

$$c_k = \frac{1}{\sqrt{N}} \sum_i c_i^+ e^{ikR_i} \quad (15)$$

$$H = \sum_k \varepsilon(k) c_k^+ c_k + \hbar\omega \sum_q a_q^+ a_q + \frac{g\hbar\omega}{\sqrt{N}} \sum_{k,q} c_k^+ c_k (a_q + a_{-q}^+) \quad (16)$$

In Eq.16  $c_k^+(c_k)$  denote electron creation (destruction) operators and  $a_q^+(a_q)$  bosonic creation (destruction) operators who accounts for phonons;  $\varepsilon(k)$  the electronic band in tight binding approximation in which we account only for superposition of atomic orbitals if they are first neighbours. Such energy of the electronic part substitutes the free particle energy of the Hamiltonian  $\left[ \varepsilon(k) = \frac{k^2}{2m} \right]$ .

Hamiltonian Eq.16 can be considered as that of Fröhlich polaron or large polaron when the bandwidth  $\varepsilon(k)$  is large enough. The application of RWA [31] to Eq.16 conducts to the appropriate form (Eq.17) of the interaction Hamiltonian, the last term to the right hand side of Eq.16 and the total Hamiltonian of the system changes to that of Eq.18.

$$\sum_{k,q} c_k^+ c_k (a_q + a_{-q}^+) = \sum_q G(q) (\sigma_- a_{-q}^+ + \sigma_+ a_q) \quad (17)$$

$$H = H_0 + \hbar\omega a^+ a + G (\sigma_- a^+ + \sigma_+ a) \quad (18)$$

The Hamiltonian of this kind has been given by [26, 27] to model decoherence in quantum computers. In Eq.18, the first term to the right hand side is the contribution of the free Qbit. The second term is the contribution of the environmental field modes alone for mode frequency  $\omega$  and  $a^+(a)$  are mode creation (destruction) operators [32]. The third term is the interaction term describing the interaction between the Qbit and the thermal field modes, with coupling  $G(q)$ . Within our simulation, we consider the phonon cloud as an atomic entity so that Eq.18 can take the best mathematical form. Under the effect of the magnetic field, the motion of the system is completely slow down. The effect of the trap is mathematically formulated through it Hamiltonian Eq.19 which has been proposed by [27] where  $\omega_B = \lambda \mu_B B$  is the corresponding magnetic field frequency,  $\lambda$  the gyromagnetic factor,  $\mu_B$  the Bohr magneton and  $B$  the magnetic field.

$$H_B = \frac{\omega_B}{2} \sigma_3 \quad (19)$$

The total Hamiltonian of the system takes the form of Eq.20 and it is called the Jaynes-Cumming Hamiltonian [27, 31].

$$H = H_0 + \hbar \omega a^\dagger a + G(\sigma_- a^\dagger + \sigma_+ a) + \frac{\omega_B}{2} \sigma_3 \quad (20)$$

Following the mathematical formalism of [27], the Hamiltonian Eq.20 becomes as given in Eq.21 if we ignore the scalar term  $\frac{E_0 + E_1}{2} I$  for simplicity where the parameter  $\Delta = \omega_B - \omega_0$  and  $\omega_0$  is the transition energy between the lower  $|0\rangle$  and upper  $|1\rangle$  energy states at unit  $\hbar$ .

$$H = \frac{\Delta}{2} \sigma_3 + \hbar \omega a^\dagger a + G(\sigma_- a^\dagger + \sigma_+ a) \quad (21)$$

It is possible to solve the Schrödinger Eq.22 for a wave function  $\psi = a\psi_0 + b\psi_1$  where  $a$  and  $b$  are transition probability amplitudes given the Hamiltonian of the type Eq.21 in the Fock space  $F$  being the Hilbert space over  $C$ .

$$i \frac{\partial \psi}{\partial t} = H \psi \quad (22)$$

$$A = \begin{bmatrix} \frac{\Delta - \omega}{2} & Ga \\ Ga^\dagger & -\frac{\Delta - \omega}{2} \end{bmatrix} \quad (25)$$

$$A^2 = \begin{bmatrix} \left(\frac{\Delta - \omega}{2}\right)^2 + G^2 aa^\dagger & 0 \\ 0 & \left(\frac{\Delta - \omega}{2}\right)^2 + Ga^\dagger a \end{bmatrix} \quad (26)$$

$$e^{-itA} = \begin{bmatrix} \cos t(\sqrt{\eta + G^2}) - i \frac{\delta}{2} \frac{\sin t(\sqrt{\eta + G^2})}{\sqrt{\eta + G^2}} & -iG \frac{\sin t(\sqrt{\eta + G^2})}{\sqrt{\eta + G^2}} a \\ -G \frac{\sin t(\sqrt{\eta})}{\sqrt{\eta}} a^\dagger & \cos t\sqrt{\eta} + i \frac{\delta}{2} \frac{\sin t(\sqrt{\eta})}{\sqrt{\eta}} \end{bmatrix} \quad (27)$$

From Eq.27, the solution to the Schrödinger Eq.24 is given by Eq.28.

$$|\phi(t)\rangle = \begin{bmatrix} \cos t(\sqrt{\eta + G^2}) - i \frac{\delta}{2} \frac{\sin t(\sqrt{\eta + G^2})}{\sqrt{\eta + G^2}} & -iG \frac{\sin t(\sqrt{\eta + G^2})}{\sqrt{\eta + G^2}} a \\ -G \frac{\sin t(\sqrt{\eta})}{\sqrt{\eta}} a^\dagger & \cos t\sqrt{\eta} + i \frac{\delta}{2} \frac{\sin t(\sqrt{\eta})}{\sqrt{\eta}} \end{bmatrix} |\phi(0)\rangle \quad (28)$$

From the initial transformation set  $|\phi\rangle = U|\psi\rangle$ , then the system's wavefunction is given in Eq.29.

To illustrate our model based on Eq.22 given Hamiltonian Eq.21, we first consider a unitary operator  $U = U(t)$  and set  $|\phi\rangle = U|\psi\rangle$  in order to show how Eq.22 can be simplified into the non linear Schrödinger equation  $i \frac{\partial |\phi\rangle}{\partial t} = \left( U H U^{-1} + i \frac{\partial U}{\partial t} U^{-1} \right) |\phi\rangle$ . If we further let  $U(t)$  as given in Eq.23, then simple calculation conducts to the pure Schrödinger Eq.24.

$$U(t) = e^{it \frac{\omega}{2} \sigma_3} \otimes e^{it \omega N} \quad (23)$$

$$i \frac{\partial |\phi\rangle}{\partial t} = \begin{bmatrix} \frac{\Delta - \omega}{2} & Ga \\ Ga^\dagger & -\frac{\Delta - \omega}{2} \end{bmatrix} |\phi\rangle \quad (24)$$

To simplify our calculations, we consider Eq.25 given that Eq.26 is verified. We can then arrive to the expression of  $e^{-itA}$  based on RWA formalism Eq.27 where  $\delta = \Delta - \omega$  and  $\eta = \frac{\delta^2}{4} + G^2 N$ .

$$|\psi(t)\rangle = \begin{bmatrix} e^{it\left(\omega N + \frac{\omega}{2}\right)} & 0 \\ 0 & e^{it\left(\omega N - \frac{\omega}{2}\right)} \end{bmatrix} \times \begin{bmatrix} \cos t\left(\sqrt{\eta+G^2}\right) - i\frac{\delta}{2}\frac{\sin t\left(\sqrt{\eta+G^2}\right)}{\sqrt{\eta+G^2}} & -iG\frac{\sin t\left(\sqrt{\eta+G^2}\right)}{\sqrt{\eta+G^2}}a \\ -iG\frac{\sin t\left(\sqrt{\eta}\right)}{\sqrt{\eta}}a^+ & \cos t\sqrt{\eta} + i\frac{\delta}{2}\frac{\sin t\left(\sqrt{\eta}\right)}{\sqrt{\eta}} \end{bmatrix} |\psi(0)\rangle \quad (29)$$

In this study, we limit ourselves to the initial conditions  $|\psi(0)\rangle = \begin{pmatrix} 1 \\ 0 \end{pmatrix} \otimes |0\rangle$  for the wavefunction  $\psi$ . Within this regime, the transition probability amplitudes  $a$  and  $b$  take the expressions given in Eq.30 and Eq.31.

$$a(t) = \exp\left(-it\frac{\omega}{2}\right) \left\{ \cos t\left(\sqrt{\eta+G^2}\right) - i\frac{\delta}{2}\frac{\sin t\left(\sqrt{\eta+G^2}\right)}{\sqrt{\eta+G^2}} \right\} \quad (30)$$

$$b(t) = -i\frac{G}{\sqrt{\eta}} \exp\left\{-it\frac{\omega}{2}\right\} \sin t\left(\sqrt{\eta}\right) \quad (31)$$

From the above transition probability amplitudes, the probability of finding the electron coupled with phononic modes is given by Eq.32 following the mathematical analysis of [26].

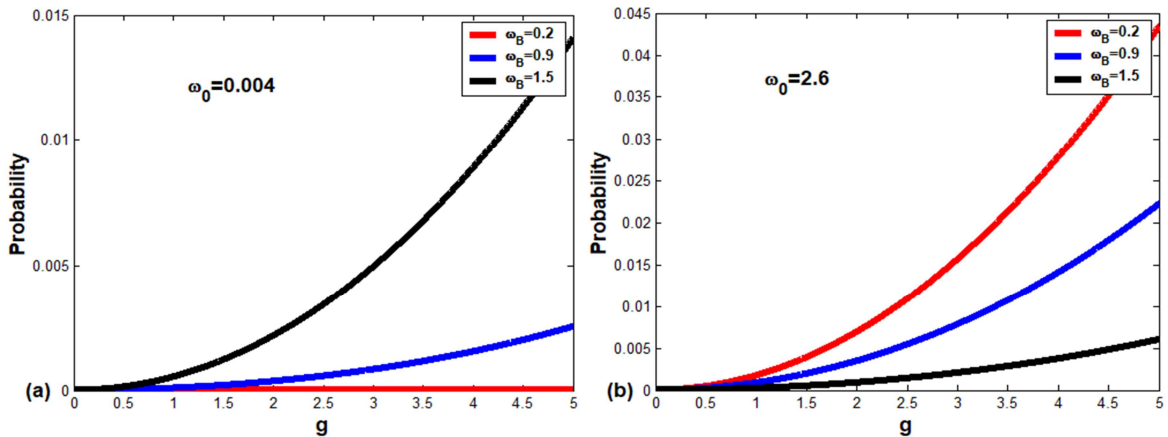
$$P = \frac{G^2}{2\eta} \left[ 1 - \cos\left(2\sqrt{\eta}t\right) \right] \quad (32)$$

According to the Schmidt decomposition, it is possible to calculate the Von Neumann entropy which characterizes the decoherence state of the system as revealed the authors of Ref. [27]. Theoretically, following the Schmidt decomposition, the entropy of the system takes the form of Eq.33 where  $a$  and  $b$  are the same transition probability amplitudes Eq.15 and Eq.16 respectively.

$$S = -|a|^2 \ln|a|^2 - |b|^2 \ln|b|^2 \quad (33)$$

### 3. Numerical Results and Discussions

In this section, we numerically discussed the influence of surrounding environment on the dynamic of cooled and trapped polaron for bandgap energies values used in experimental studies of [33-36]: (a)  $\omega_0 = 0.004$  [33]; (b)  $\omega_0 = 2.6$  [34]; (c)  $\omega_0 = 3.5$  [35] and (d)  $\omega_0 = 12.5$  [36]. The cooled and trapped polaron will be call for simplicity polaron. We begin with the graphical representation (Figure 1) of the density of the population in the excited state versus coupling strength constant for some values of magnetic field frequency in various cases of bandgap values used in different experimental studies mentioned above. We choose the parameter values  $N = 0.5$  and  $t = 1.5$ . At the beginning of the trapping process, the system is in the ground state. The probability of finding the trapped polaron in the excited state increases with coupling strength constant. The dynamic of the polaron is controled by the surrounding phononic environment. Such a result has been observed by [26] in the case of polariton. The result is due to the BDPEP as predicted by [37] and confirmed by [38]. The polaron behaves alike to the polariton under cooling and trapping processes with magnetic field. The figure (Figure 1) shows that the effet of the trap on the system is a function of coupling strength constant  $g$ . Coherent population transfert from ground to excited state is observed if the bandgap energy value of the system is neither too low nor too high (Figure 1c).



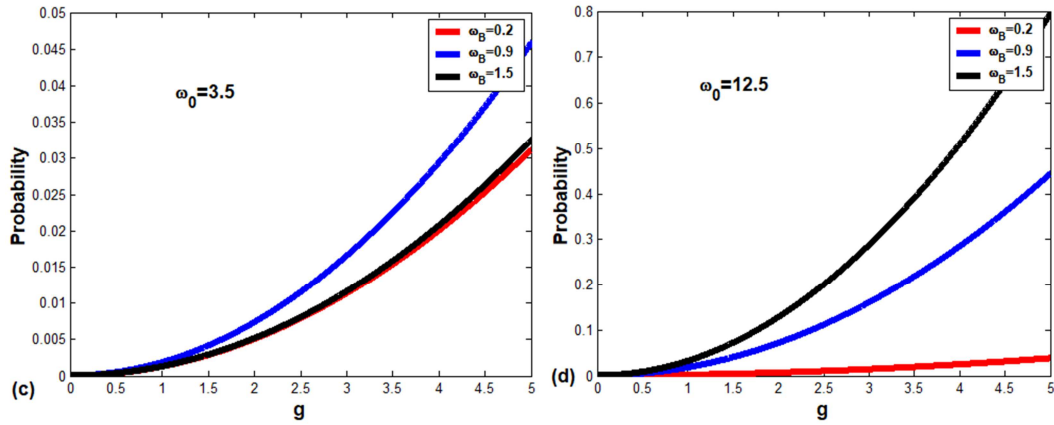


**Figure 1.** Transition probability versus coupling strength constant for some values of magnetic field frequency in various cases of bandgap values used in different experimental studies: (a)  $\omega_0 = 0.004$  [33]; (b)  $\omega_0 = 2.6$  [34]; (c)  $\omega_0 = 3.5$  [35]; (d)  $\omega_0 = 12.5$  [36]. Here, the parameter value  $N = 0.5$  and  $t = 1.5$ .

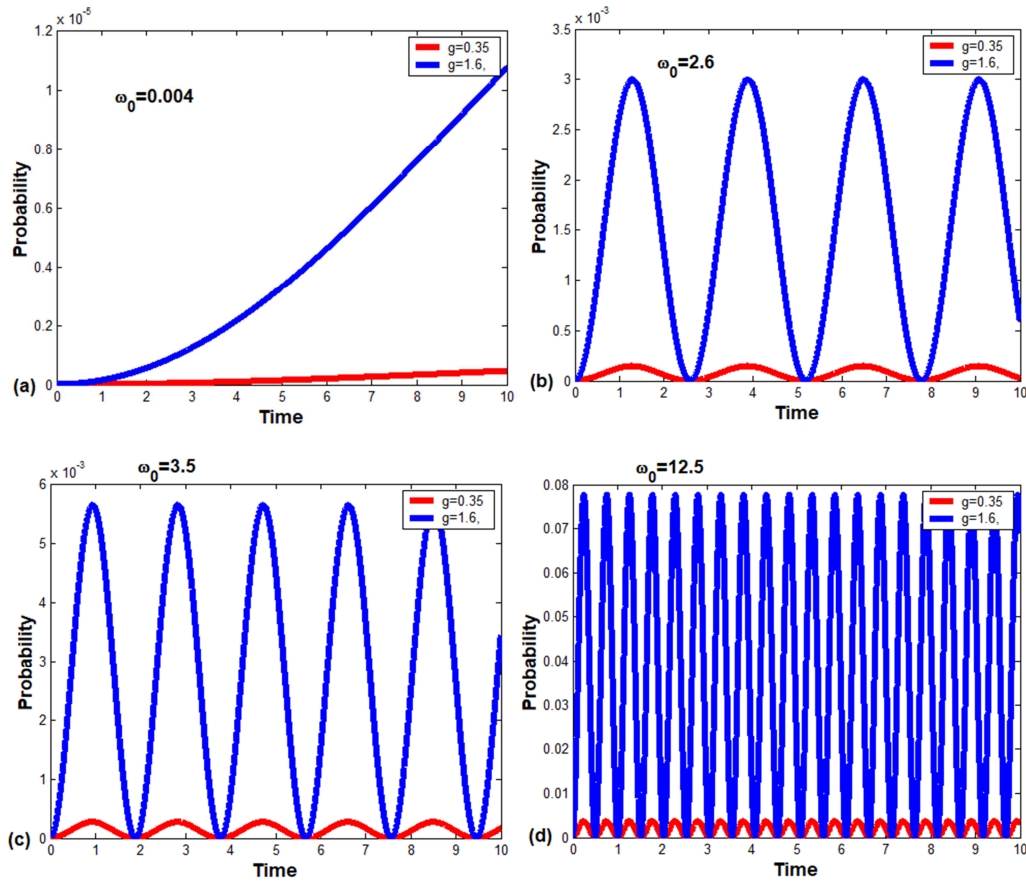


**Figure 2.** Transition probability versus time for some values of magnetic field frequency in various cases of bandgap values used in different experimental studies at both low ( $g = 0.35$ ) and strong ( $g = 1.6$ ) coupling strength constant: (a)  $\omega_0 = 0.004$  [33]; (b)  $\omega_0 = 2.6$  [34]; (c)  $\omega_0 = 3.5$  [35]; (d)  $\omega_0 = 12.5$  [36]. Here, other parameter values are  $N = 0.5$  and  $\omega = 0.02$ .

In Figure 2, the parameter of interest is the cooling and trapping time. We depicted transition probability versus time for some values of magnetic field frequency in various cases of energy bandgap values at both low ( $g = 0.35$ ) and strong ( $g = 1.6$ ) coupling regime. The values of  $g < 1$  and  $g = 1.6$  have been identified by [26] as being in the low and strong coupling strength constant respectively in the Rabi model. No matter their study has been focused on polariton, we also

find interesting to use the values in the present study for the reason which is being already mentioned in the former paragraph. Figure 2 presents Rabi oscillation which is in accordance with the result of [26]. Very long time cooling and trapping process conducts to interferences. This is observed through an increasing number of Rabi oscillation. The cooled and trapped polaron manifest itself as being potential candidate for interferometry applications.



Transition probability versus magnetic field frequency is depicted in Figure 3 for various cases of bandgap values [33-36] at both low ( $g = 0.35$ ) [Figure 3a] and strong ( $g = 1.6$ ) [Figure 3b] coupling strength constant respectively. The figure shows the dependance of transition probability to the intrinsic parameter of the trap, i.e magnetic field frequency. We observe that without cooling and trapping process, the probability of finding the polaron in the excited state is very important. This result is in accordance to that of [27]. The probability of finding the polaron in the excited state decreases progressively with magnetic field frequency. Thus, trapping conducts to complete population transfer from excited state to ground state with the possibility of the formation of BEC at bot low bandgap energy values and important value magnetic field frequency. In contrast, when the bandgap energy value is too important ( $\omega_0 = 12.5$ ), we observe another behaviour of the system, when the magnetic field frequency is beyond  $\omega_B = 0.2$ , leading to a phenomenon which seems like complete population transfer from ground to excited state. The explanation which comes from such a result is that, due to strong magnetic field, ionized particles associated to free electrons do not conduct to cooling and trapping of atomic entities, but instead plasma formation [39]. The observed evolution of transition probability in term of magnetic field frequency when the bandgap energy is very important can be interpreted in terms of quasiparticles scattering. This result, which stands as one of our best result, complete the shortcomings observed in the research works of [26, 27].

In Figures 4-6, we schematically depicted the Von Neumann entropy of the system againts time [Figure 4], coupling strength constant [Figure 5] and magnetic field [Figure 6]. It is evident that the entropy makes almost periodic oscillation [Figure 4]. This means that the magnetic field can be use to help to realize and stabilize the degree of entanglement between the polaron and the field at a high level. Sometimes [Figure 4 (a-c)], for low bandgap energy, the polaron field system becomes paramountly entangled. We find that the entanglement can last a longer time as the system of cooled and trapped polaron is strongly coupled with the trap. The entanglement decays to the asymptotic value in both larger values of coupling strength constant and photon's frequency. So far, it's observes that these figures seems like those obtain by authors of Ref. [40]. To properly

illustrate how the trap influences the dynamic of polaron, the response of entropy versus coupling strength constant is shown in Figure 5 for differents values of magnetic field and in various cases of bandgap energy values [33-36]. At low interaction system-environment and for different values of magnetic field intensity, almost nothing happens in the system. The entropy is the linear evolution of the coupling strength  $g$ . Around the value  $g = 1.6$  the entropy exhibits a power law decay. The linear phase is an indication of the energy shift of the polaron state. Yields the formation of repulsive or upper polaron (UP) and attractive or lower polaron (LP). The parabolic transient stands for the ultrafast cooled and trapped polaron formation. Following the analysis of [38], the observation of both repulsive and attractive quasiparticles branches of cooled and trapped polaron energy predicts the possibility of formulating Landau Zener (LZ) problem in magnetic cooling and trapping of polaron. The strong coupling dynamic of polaron is universal, as it is for systems with different experimental bandgap values [33-36]. Finally, the entropy behaves as similar as the Ramsey contrast associated with orthogonality catastrophe. The phenomnon was originally studied in the context of x-ray absorption spectra in metals, where high-energy x-ray photons create atomic core holes by photoemission of inner-shell electrons. Today, it is a challenge for theoretical approaches to investigate an exact solution of orthogonality catastrophe. However, theoretical analysis based on magnetic trapping of atomic entities such as polaron would be ideally suited to probe the competition between these effects. For the lowest and strongest possible interactions with surrounding environment, a description of the dynamic of cooled and trapped polaron with magnetic field in terms of entropy is depicted in Figure 6 as a function of magnetic field. For intermediate bangap energy values, i.e  $\omega_0 = 2.6$  [34] and (c)  $\omega_0 = 3.5$  [35], the increase in the magnetic field leads to the decrease in entropy reaching almost zero which indicates the formation of BEC. In contrast, for lower bandgap energy, an increase in the magnetic field conducts to the destruction of the coherent state of the system. Meanwhile, in the regime of important value bandgap energy, the same interpretation is given as in the case of Figure 3.

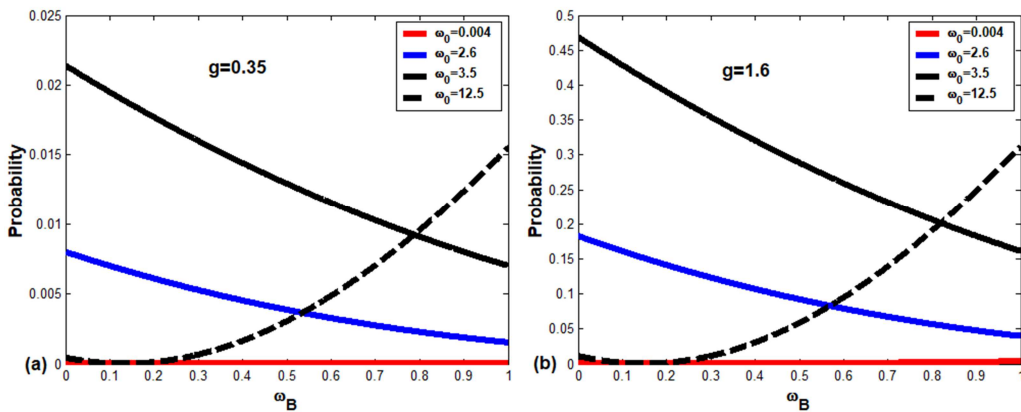


**Figure 3.** Transition probability versus magnetic field frequency for various cases of bandgap values used in different experimental studies at both low ( $g = 0.35$ ) (a) and strong ( $g = 1.6$ ) (b) coupling strength constant respectively.

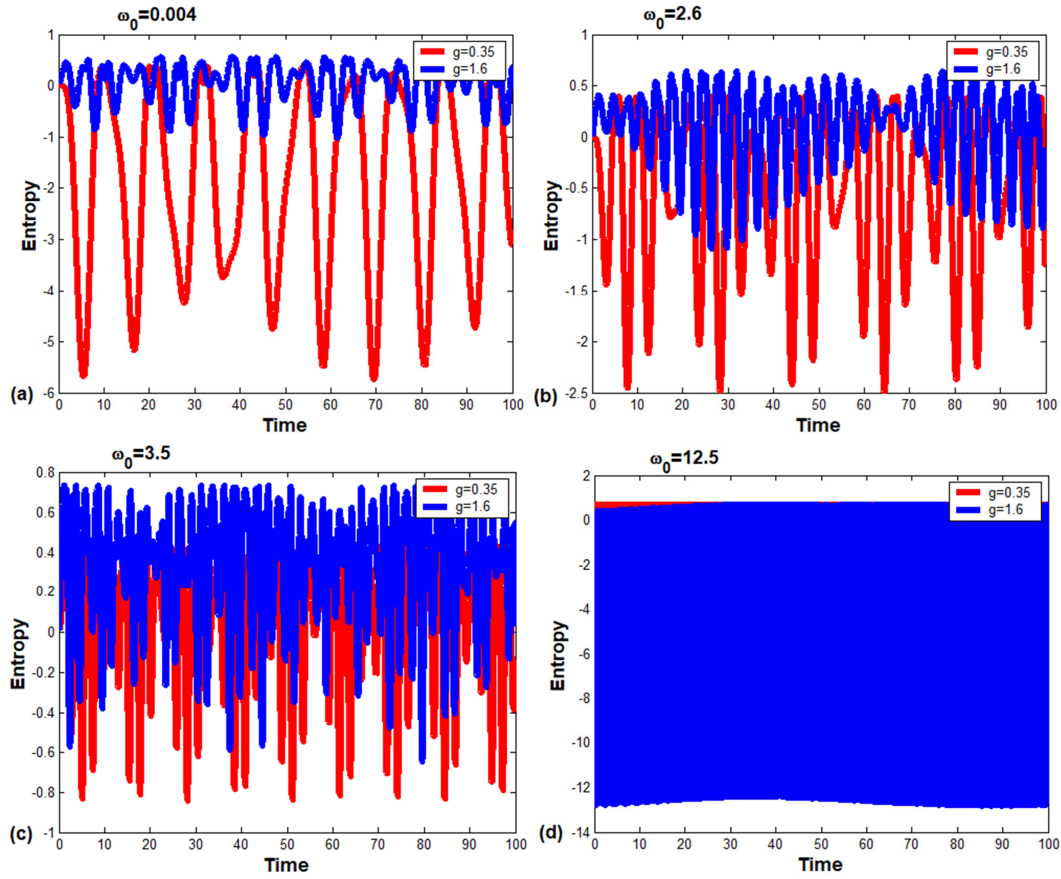


**Figure 4.** Graphical representation of entropy versus time for various cases of bandgap values used in different experimental studies at both low ( $g=0.35$ ) (a) and strong ( $g=1.6$ ) (b) coupling strength constant respectively.

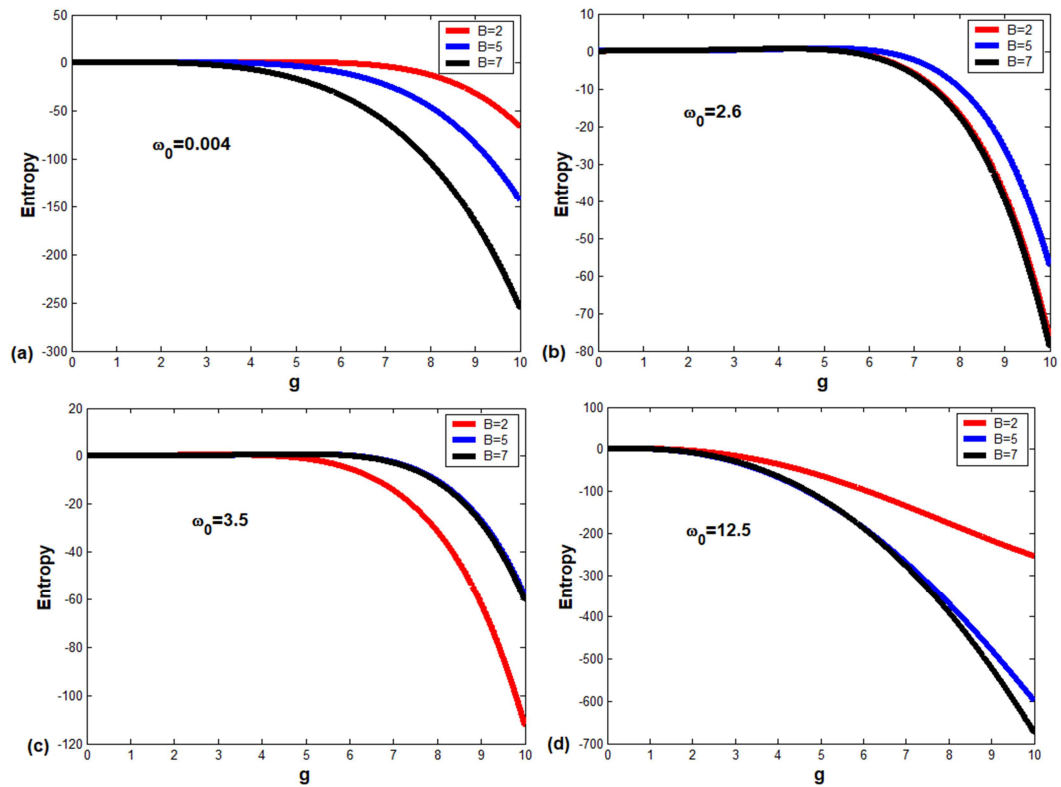


**Figure 5.** Entropy versus coupling strength constant for some values of magnetic field  $B$  for various cases of bandgap values used in different experimental studies.



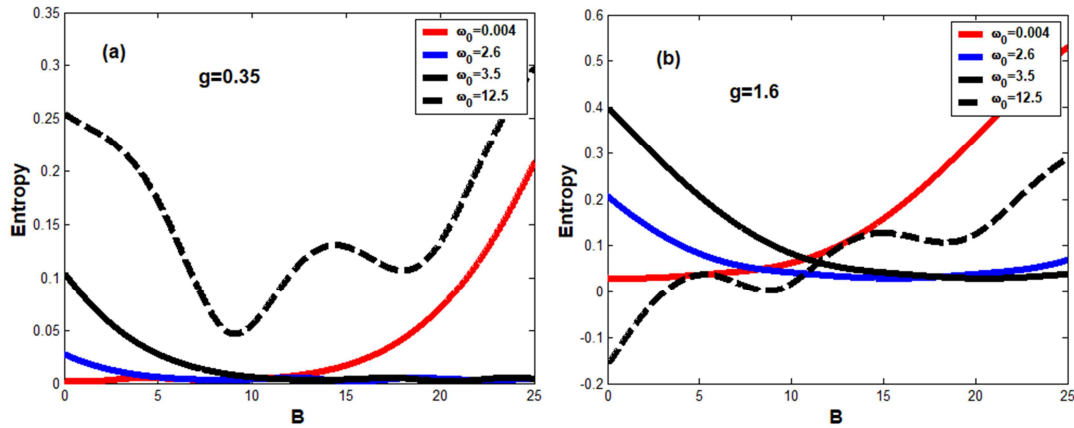


**Figure 6.** Entropy versus magnetic field  $B$  for various cases of bandgap values used in different experimental studies at both low ( $g = 0.35$ ) (a) and strong ( $g = 1.6$ ) (b) coupling strength constant respectively.

## 4. Conclusion

In summary, we have investigated the influence of magnetic trap on the dynamic of electron coupled with phononic modes originated by a lattice of diatomic molecules. Under semi-classical approach, we evaluated transition probabilities and Von Neumann entropy using RWA. Through theoretical analysis, we consider the polaritonic entity as being a TLS. We found that, trapping of Fröhlich polarons with magnetic field conducts to complete population transfer from excited state to ground state with the possibility of the formation of BEC at both low bandgap energy values and important value magnetic field frequency. Moreover, despite the BDPEP, the magnetic trapping of quasiparticles Fröhlich polarons conducts to plasma formation when both the bandgap value of energy levels and the magnetic field frequency are very important. At low coupling with surrounding environment the entropy is the linear evolution of the coupling strength  $g$  which corresponds to the energy shift of the polaron state with consequences the formation of UP and LP which predict the possibility of formulating LZ problem in cooling and trapping of polaron. In contrast, around the value  $g = 1.6$ , the entropy exhibits a power law decay. The entropy behaves as similar as the Ramsey contrast associated with orthogonality catastrophe, meaning that cooled and trapped polarons are suited candidate to provide insight into theoretical analysis in orthogonality catastrophe questions based.

## References

- [1] Klein, E. La physique quantique et ses interpretations. SER, 5, Tome 394, (2001): 629-639. DOI: 10.3917/etu.945.0629.
- [2] Benioff, P. The computer as a physical system: a microscopic quantum mechanical Hamiltonian model of computers as represented by Turing machines. J Stat Phys 22, (1980): 563-591. DOI: <https://doi.org/10.1007/BF01011339>.
- [3] Feynman, R. P. Simulating Physics with computers. Int. J. Theor. Phys. 21, (1982): 467-488. DOI: <https://doi.org/10.1007/BF02650179>.
- [4] Shor, P. W. Algorithms for quantum computation: discrete logarithms and factoring. 35th Symposium on the Foundations of Computer Science, New Mexico, 20-22 November 1994, (1994): 124-134. DOI: <http://dx.doi.org/10.1109/SFCS.1994.365700>.
- [5] Strunz, W. T., Haake, F., Braun, D. Universality of decoherence for macroscopic quantum superpositions. Physical Review A, 67 (2), 022101, (2003): 1-13. DOI: 10.1103/PhysRevA.67.022101.
- [6] Burkard, G., Loss, D., DiVincenzo, D. P. Coupled quantum dots as quantum gates, Phys. Rev. B 59, (1999): 2070-2078. DOI: <https://doi.org/10.1103/PhysRevB.59.2070>.
- [7] Leroyer, Y., Sénizergues, G. Introduction à l'information quantique. ENSEIRB-MATMECA. Polycopié du Calcul quantique. (2016). 110 Pges.
- [8] Chuang, I. L., Yamamoto, Y. A Simple Quantum Computer. Phys. Rev. A, 52, (1995): 3489-3496. DOI: <https://doi.org/10.1103/PhysRevA.52.3489>.
- [9] Deutsch, D. Quantum computational networks, Proc. R. Soc. Lond. A, 425, (1989): 73-90. DOI: 10.1098/rspa.1989.0099.
- [10] Steane, A. Quantum computing. Rep. Prog. Phys 61, (1998): 117-173. DOI: <http://dx.doi.org/10.1088/0034-4885/61/2/002>.
- [11] Ekert, A., Jozsa, R. Quantum computation and Shor's factoring algorithm. Rev. Mod. Phys 68, (1996): 733-753. DOI: <https://doi.org/10.1103/RevModPhys.68.733>.
- [12] Spiller, T. P. Quantum information processing: cryptography, computation and teleportation. Proc. IEEE, 84 (12), (1996): 1719-1746. DOI: 10.1109/5.546339.
- [13] Benioff, P. Models of quantum turing machines. Fortschr. Phys, 46 (4-5), (1998): 423-441. DOI: [https://doi.org/10.1002/\(SICI\)1521-3978\(199806\)46:4/5<423::AID-PROP423>3.0.CO;2-G](https://doi.org/10.1002/(SICI)1521-3978(199806)46:4/5<423::AID-PROP423>3.0.CO;2-G).
- [14] Kielpinski, D., Monroe, C., Wineland, D.J. Architecture for a large-scale ion-trap quantum computer. Nature 417, (2002): 709-711. DOI: <https://doi.org/10.1038/nature00784>.
- [15] Shor, P. W. Scheme for reducing decoherence in quantum computer memory. Phys. Rev. A 52, (1995): R2493-R2496. DOI: <https://doi.org/10.1103/PhysRevA.52.R2493>.

- [16] Roszak, K., Filip, R., Novotny, T. Decoherence control by quantum decoherence itself. *Sci. Rep* 5, 9796 (2015): 1-10. DOI: <https://doi.org/10.1038/srep09796>.
- [17] Ban, M. Photon-echo technique for reducing the decoherence of a quantum bit. *Journal of Modern Optics*, 11 (45), (1998): 2315-2325. DOI: <https://doi.org/10.1080/09500349808231241>.
- [18] Calderbank, A. R., Shor, P. W. Good quantum error-correcting codes exist. *Phys. Rev. A* 54 (2), (1996). 1098-1105. DOI: 10.1103/PhysRevA.54.1098.
- [19] Laflamme, R., Miquel, C., Paz, J. P., Zurek, W. H. Perfect quantum error correcting code. *Phys. Rev. Lett.* 77 (1). (1996): 198-201. DOI: 10.1103/PhysRevLett.77.198.
- [20] Steane, A. M. Error correcting codes in quantum theory. *Phys. Rev. Lett.* 77 (5), (1996): 793-797. DOI: 10.1103/physrevlett.77.793.
- [21] Chuang, I. L., Yamamoto, Y. Creation of a persistent quantum bit using error correction. *Phys. Rev. A*, 55 (1), (1997): 114-127. DOI: 10.1103/PhysRevA.55.114.
- [22] Knill, E., Laflamme, R. Theory of quantum error-correcting codes. *Phys. Rev. A*, 55 (2). (1997): 900-911. DOI: 10.1103/PhysRevA.55.900.
- [23] Braunstein, S. L., Smolin, J. A. Perfect quantum-error-correction coding in 24 laser pulses. *Phys. Rev. A*, 55 (2), (1997): 945-950. DOI: <https://doi.org/10.1103/PhysRevA.55.945>.
- [24] Fotue, A. J., Djomou, D. R.-J., Kenfack, S. C., Fobasso, M. F. C., Fai, L. C. Stability and decoherence of optical bipolaron in symmetric quantum dot. *Eur. Phys. J. Plus*: (2020): 1-14. DOI: 10.1140/epjp/s13360-020-00835-5.
- [25] Nguenang, P., Jipdi, N. M., Louodop, P., Tchoffo, M., Fai, L. C., Cerdeira, H. A. Quantum interferometry for different energy Landscape in a tunable Josephson-junction circuit. *Journal of Applied Mathematics and Physics*, 8, (2020): 2569-2600. DOI: 10.4236/jamp.2020.81192.
- [26] Kenfack, S. C., Ekengoue, C. M., Fotue, A. J., Fobasso, F. C., Bawe Jr, G. N., Fai, L. C. Laser cooling and trapping of polariton. *Computational Condensed Matter* 11, (2017): 47-54. DOI: <http://dx.doi.org/10.1016/j.cocom.2017.05.001>.
- [27] Ekengoue, C. M., Kenfack, S. C., Fotue, A. J., Fobasso, M. F. C., Bawe Jr, G. N., Fai, L. C. Decoherence of cooled and trapped polariton under magnetic field. *Computational Condensed Matter* 14, (2018): 106-113. DOI: <https://doi.org/10.1016/j.cocom.2018.01.012>
- [28] Brandt, H. E. Qubit devices and the issue of quantum decoherence. *Progress in Quantum Electronics*, 22 (5-6), (1998): 257-370. DOI: [https://doi.org/10.1016/S0079-6727\(99\)00003-8](https://doi.org/10.1016/S0079-6727(99)00003-8).
- [29] Monroe, C., Meekhof, D. M., King, B. E., Itano, W. M., Wineland, D. J. (1995). Demonstration of a fundamental quantum logic gate. *Phys. Rev. Lett.* 75 (25), (1995): 4714-4717. DOI: 10.1103/physrevlett.75.4714.
- [30] Devreese, J. T. Fröhlich polarons from 3D to 0D: concepts and recent developments (Part I), 2005, P.186.
- [31] Fujii, K. Introduction to the Rotating Wave Approximation (RWA): Two coherent oscillations. *Journal of Modern Physics*, 8, (2017): 2042-2058. DOI: 10.4236/jmp.2017.812124.
- [32] Walls, D. F., Milburn, G. J. *Quantum Optics*, Springer-Verlag, Berlin, (1994). ISBN: 978-3-540-28574-8.
- [33] Oliver, W. D., Yu, Y., Lee, J. C., Berggren, K. K., Levitov, L. S., Orlando, T. P. Mach-Zehnder interferometry in a strongly driven superconducting qubit. *Science*, 9 (310). (2005): 1653-1657. DOI: 10.1126/science.1119678.
- [34] Wilson, C. M., Duty, T., Persson, F., Sandberg, M., Johansson, G., Delsing, P. Coherence times of dressed states of a superconducting qubit under extreme driving. *Phys. Rev. Lett.* 98, 257003, (2007): 1-4. DOI: 10.1103/PhysRevLett.98.257003.
- [35] Izmalkov, A., Van der Ploeg, S. H. W., Shevchenko, S. N., Grajcar, M., Il'ichev, E., Hübner, U., Omelyanchouk, A. N., Meyer, H.-G. Consistency of ground state and spectroscopic measurements on flux qubits. *Phys. Rev. Lett.* 101 (1). 017003, (2008): 1-4. DOI: 10.1103/PhysRevLett.101.017003.
- [36] Sillanpää, M., Lehtinen, T., Paila, A., Makhlin, Y., Hakonen, P. Continuous-time monitoring of Landau Zener interference in a cooper-pair Box. *Phys. Rev. Lett.* 96, 187002, (2006): 1-4. DOI: <https://doi.org/10.1103/PhysRevLett.96.187>.
- [37] Matthews, C. F. J., Poullos, K., Meinecke, J. D. A., Politi, A., Peruzzo, A., Ismail, N., Wörhoff, K., Thompson, M. G., O'Brien, J. L. (2013). *Sci. Rep.* 1539 (3), 1-6.
- [38] Kenfack-Sadem, C., Ekengoue, C. M., Danga, J. E., Fotue, A. J., Fobasso, M. F. C., Fai, L. C. Lasser control of polariton using Landau-Zener-Stückelberg interferometry theory. *The European Physical Journal Plus* 135, 815, (2020): 1-24. DOI: <https://doi.org/10.1140/epjp/s13360-020-00790-1>.
- [39] Langmuir, I. Oscillations in ionized gases. *Proceedings of the National Academy of Science*, 14 (8), (1928): 627-637. DOI: 10.1073/pnas.14.8.627.
- [40] Kenmoe, M. B., Mkam Tchouobiap, S. E., Danga, J. E., Kenfack Sadem, C., Fai, L. C. Lie algebras for some specific dissipative Landau-Zener problems. *Physics Letters A*, 379 (7), (2015): 635-642. DOI: <https://doi.org/10.1016/j.physleta.2014.12.032>.